Mitochondrial delivery of antisense RNA by MITO-Porter results in mitochondrial RNA knockdown, and has a functional impact on mitochondria

Ryo Furukawa[a,b], Yuma Yamada[a,b], Eriko Kawamura[a], and Hideyoshi Harashima[a]*

[a] Laboratory for molecular design of pharmaceutics, Faculty of Pharmaceutical Sciences, Hokkaido University, Kita-12, Nishi-6, Kita-ku, Sapporo, 060-0812, Japan

[b] The first two authors contributed equally as joint First Authors

*Corresponding author: Laboratory for molecular design of pharmaceutics, Faculty of Pharmaceutical Sciences, Hokkaido University, Kita-12, Nishi-6, Kita-ku, Sapporo 060-0812, Japan

Tel: +81-11-706-3919 Fax: +81-11-706-4879 E-mail: harasima@pharm.hokudai.ac.jp

Abstract

Mitochondrial genome-targeting nucleic acids are promising therapeutic candidates for treating mitochondrial diseases. To date, a number of systems for delivering genetic information to the cytosol and the nucleus have been reported, and several successful gene therapies involving gene delivery targeted to the cytosol and the nucleus have been reported. However, much less progress has been made concerning mitochondrial gene delivery systems, and mitochondrial gene therapy has never been achieved. Here, we report on the mitochondrial delivery of an antisense RNA oligonucleotide (ASO) to perform mitochondrial RNA knockdown to regulate mitochondrial function. Mitochondrial delivery of the ASO was achieved using a combination of a MITO-Porter system, which contains mitochondrial fusogenic lipid envelopes for mitochondrial delivery via membrane fusion and D-arm, a mitochondrial import signal of tRNA to the matrix. Mitochondrial delivery of the ASO induces the knockdown of the targeted mitochondria-encoded mRNA and protein, namely cytochrome c oxidase subunit II, a component of the mitochondrial respiratory chain. Furthermore, the mitochondrial membrane potential was depolarized by the down regulation of the respiratory chain as the result of the mitochondrial delivery of ASO. This finding constitutes the first report to demonstrate that the nanocarrier-mediated mitochondrial genome targeting of antisense RNA effects mitochondrial function.

1. Introduction

Small interfering RNA (siRNA) is frequently used to achieve specific knockdown of target mRNA [1]. Although recent studies have addressed the component of the RNA-induced silencing complex in mitochondria, applications of siRNA to mitochondria have not been reported [2]. On the other hand, this unique organelle possesses not only protein-coding mRNA transcribed from mitochondrial DNA (mtDNA) but also non-coding RNAs such as tRNA, rRNA, and microRNA (miRNA) [3-8]. It has been reported that miRNAs have the potential to regulate mitochondrial gene expression via a post-transcriptional pathway such as mitochondrial RNA degradosomes [9-12]. Thus, the knockdown of mitochondrial RNA via the mitochondrial delivery of antisense RNA oligonucleotide (ASO) would be expected to contribute to the development of a mitochondrial therapeutic approach and a more complete understanding of the post-transcriptional regulation.

System for nucleic acids targeted to the cytosol and nucleus have been reported, while less efforts have been expended on mitochondrial delivery systems [1, 13, 14]. Weissig *et al* reported that DQAsome, the mitochondriotropic nanocarrier [15, 16], was useful in altering mitochondrial gene expression by virtue of delivering a mini-mitochondrial genome to mitochondria [16]. However, a universal carrier has not yet been developed for mitochondrial matrix delivery, although they reported that an approach using a cationic nanocarrier such as DQAsome could be useful in terms of interacting with mitochondria. Seibel *et al* reported that oligo DNA (ODN) and a peptide nucleic acid (PNA) covalently conjugated with the mitochondrial targeting signal peptide (MTS) can be introduced into isolated mitochondria [17, 18]. With the help of a device the cytoplasmic delivery, MTS-conjugated PNA was imported into mitochondria in cells. This method could be a viable strategy for the genetic modification of mitochondria [18]. We recently

developed a MITO-Porter system, mitochondrial delivery system via mitochondrial outer membrane fusion [19, 20]. We applied the MITO-Porter system to mitochondrial genome targeting, such as the specific digestion of mtDNA by delivering encapsulated DNase I [21, 22].

In this study, we report on mitochondrial ASO delivery using an R8/GALA-modified MITO-Porter, and validation of mitochondrial RNA knockdown to control mitochondrial function. As shown in Figure 1A, the R8/GALA-modified MITO-Porter is surface-modified with a high density of octaarginine (R8), which permits the particle to be efficiently internalized by cells via macropinocytosis (1st step) [23]. Once inside the cell, the carrier escapes from the endosome into the cytosol with the assistance of GALA, a pH-sensitive membrane fusogenic peptide (2nd step) [24-26]. The carrier then binds to mitochondria via electrostatic interactions with R8 (3rd step). In this experiment, we packaged the D-arm modified ASO in the carrier. D-arm is a D stem-loop import signal of $tRNA^{Tyr}$(GUA) with the sequence UGGUAGAGC, and is efficiently imported into the mitochondrion of Leishmania, a kinetoplastid protozoan [27]. Oligo nucleic acids constituting D-arm or its analogues can also be imported into the mitochondrial matrix through the mitochondrial inner membrane in isolated mitochondria [28, 29]. Thus, it was expected that D-arm modified ASO encapsulated in the R8/GALA-modified MITO-Porter would facilitate mitochondrial matrix delivery. One possibility is that the MITO-Porter delivers the D-arm ASO to the mitochondrial intermembrane space after fusion with the outer membrane, and it is then imported into the mitochondrial matrix via the D-arm import machinery (upper part in Figure 1B). An alternate another possibility is that the carriers directly introduce ASO into the mitochondrial matrix via step-wise membrane fusion on the contact sites of the outer and inner mitochondrial membranes (lower part in Figure 1B).

We first constructed R8/GALA-modified MITO-Porter (D-arm ASO [COX II]), where D-arm modified ASO which targeted mitochondrial mRNA that codes for cytochrome c oxidase subunit II (COX II) was packaged. COX II is one of mitochondrial proteins that make up complex IV of the respiratory chain related to maintaining the mitochondrial membrane potential. If the knockdown of the COX II mRNA was successful, the expression levels of the target mitochondrial protein would be decreased, followed by a decrease in mitochondrial functions such as maintaining membrane potential (Figure 1C). The knockdown of target mitochondrial mRNA and protein were then evaluated to demonstrate the efficiency of mitochondrial ASO delivery using the R8/GALA-modified MITO-Porter using quantitative reverse transcription PCR (qRT-PCR) and immunostaining. Moreover, we evaluated the mitochondrial membrane potential to investigate the effect of the mitochondrial ASO transfection on mitochondrial function.

2. Materials and methods

2.1. Chemicals and materials

1,2-dioleoyl-sn-glycero-3-phosphoethanolamine (DOPE) and sphingomyelin (SM) were purchased from Avanti Polar lipids (Alabaster, AL). Cholesteryl hemisuccinate (CHEMS) were purchased from Sigma (St Louis, MO). Stearylated R8 and Cholesterol-GALA were obtained from KURABO Industries (Osaka, Japan). D-arm modified antisense 2′ -O-Methyl (2′-OMe) RNA which targeted COX II (D-arm ASO [COX II]) (5′-GGGACUGUAGCUCAAUUGGUAGAGCAUCUUGCGCUGCAUGUGCCAU -3′), D-arm-modified 2′-OMe RNA non-targeting COX II (D-arm Mock) (5′-GGGACUGUAGCUCAAUUGGUAGAGCAUCGACAAGCGCACCGAU -3′), D-arm-

unmodified antisense 2′-OMe RNA which targeted COX II (ASO [COX II]) (5′-CUUGCGCUGCAUGUGCCAU -3′) and D-arm-unmodified 2′-OMe RNA non-targeting COX II (Mock) (5′- CGACAAGCGCACCGAU -3′) were purchased from Hokkaido System Science Co., Ltd. (Sapporo, Japan). The properties of these RNA oligonucleotides are summarized in Table S1. Cy5-labbled D-arm ASO (COX II) were purchased from Greiner Bio-One GmbH (Kremsmuenster, Austria). HeLa human cervix carcinoma cells were obtained from the RIKEN Cell Bank (Tsukuba, Japan). Dulbecco's modified Eagle medium (DMEM) and fetal bovine serum were purchased from Invitrogen (Carlsbad, CA). The rabbit anti-cytochrome c oxidase subunit II (COX II) antibody and mouse anti-Succinate dehydrogenase complex subunit A (SDHA) monoclonal antibody were purchased from Abcam (Cambridge, UK). Alexa Fluor 488 goat anti-rabbit IgG (H+L) and Alexa Fluor 488 goat anti-mouse IgG (H+L) was purchased from Invitrogen. Carbonyl cyanide 4-(trifluoromethoxy) phenylhydrazone (FCCP) was purchased from Sigma. JC-1 was purchased from Invitrogen. Hoechst 33342 was purchased from Dojindo (Kumamoto, Japan). All other chemicals used were commercially available reagent-grade products.

2.2 Preparation of R8/GALA-modified MITO-Porter

R8/GALA-modified MITO-Porter encapsulating ASO (D-arm ASO [COX II] or D-arm Mock) was constructed by the ethanol dilution method [30]. The R8/GALA-modified MITO-Porter had a component molar ratio of DOPE/SM/stearylated R8/Chol-GALA (molar ratio: 9/2/2/0.2). The EtOH solution of the lipids (1.1 mM lipids) was titrated slowly with ASO under vigorous mixing to avoid a low local concentration of EtOH and diluted quickly with HEPES buffer to a final concentration of < 20% EtOH. The ethanol was removed by ultrafiltration,

replacing external buffer with HEPES buffer and concentrating the R8/GALA-modified MITO-Porter.

Particle diameters and polydispersity index (PDI) as an indicator of the particle-size distribution were measured using a dynamic light scattering (DLS) method (Zetasizer Nano ZS; Malvern Instruments, Worcestershire, UK). Samples were prepared in 10 mM HEPES buffer at 25°C and the values of particle diameters are shown in the form of volume distribution. The ξ-potentials of samples were also determined in 10 mM HEPES buffer at 25°C using a Zetasizer Nano ZS.

2.3 Cell cultures

HeLa cells were maintained in complete medium which is DMEM supplemented with 10% FBS, penicillin (100 units/mL), and streptomycin (100 μg/mL). The cells were cultured under an atmosphere of 5% CO_2/air at 37°C. One day before transfection, the HeLa cells were seeded on a plates or dishes for each experiment. Immediately before transfection, the medium was replaced to serum-free medium, DMEM unsupplemented with antibiotics.

2.4 Quantification of target mitochondrial mRNA levels

R8/GALA-modified MITO-Porter encapsulating ASO (D-arm ASO [COX II] or D-arm Mock) (50-250 nM of total ASOs) were incubated with HeLa cells (5 x 10^4 cells/dish) seeded on 12-well plate in 1 mL of serum free DMEM for 3 hr under an atmosphere of 5 % CO_2/air at 37°C.

The cells were washed with phosphate-buffered saline (PBS), and further incubated in complete medium for 21 hr. Total RNA (500 ng) was purified with RNeasy (Qiagen, Hilden, Germany) according to the manufacture's protocol, combined with DNase I digestion for the degradation of DNA in total RNA samples using TURBO DNase treatment and removal reagents [Ambion by Life Technologies, Carlsbad, CA, USA]. The resulting RNA suspension was reverse transcribed using a High Capacity RNA-to-cDNA kit (Applied Biosystems, Foster City, CA) according to the manufacturer's protocol. A quantitative PCR analysis was performed on cDNA using SYBR Green Realtime Master Mix (Takara, Shiga, Japan) and Stratagene MX3005P (Agilent Technologies; Santa Clara, CA). All reactions were performed at a volume of 25 μL. The primers for mitochondrial mRNA coding COX II (target mRNA) were (forward) 5′-ATCATCCTAGTCCTCATCG -3′ and (reverse) 5′- GATTTGATGGTAAGGGAGG -3′ and for mitochondrial mRNA coding NADH dehydrogenase subunit I (ND I) (control mRNA) were (forward) 5′- TTCCTAATGCTTACCGAACG -3′ and (reverse) 5′-GGTGAAGAGTTTTATGGCGT -3′. Relative COX II/NDI mRNA expression levels were calculated as the amounts of DNA derived from COX II mRNA divided by the amounts of DNA derived from ND I mRNA.

We confirmed the absence of contaminating DNA when this RT–PCR assay was peformed. Gel images of RT–PCR detection showed that the target DNA bands appeared in the case of reverse transcription (RT(+)) (lanes 2,3 in Figure S1) and they disappeared in the absence of reverse transcription (RT(-)) (lanes 4,5 in Figure S1). We also observed the same tendency when qRT-PCR was performed (data not shown). It was confirmed that RT–PCR with specific primers for mitochondrial mRNA coding COX II could detect single bands coresponding to the target mRNA (lanes 2,3 in Figure S1).

2.5 Intracellular observation of R8/GALA-modified MITO-Porter encapsulating fluorescent labeled ASOs using confocal laser scanning microscopy (CLSM)

The R8/GALA-modified MITO-Porter encapsulating Cy5-labeled ASO (75 nM of total ASOs) was incubated with HeLa cells (1 x 10^5 cells/mL) seeded on 35 mm dishes (IWAKI, Osaka, Japan) in 1 mL of serum free DMEM for 1 hr at 37°C, and further incubated in complete medium for 2 hr. Lipofectamine (LFN) RNAi MAX (Invitrogen), as a control was used according to the manufacturer's protocol. The cells were observed by CLSM after staining the mitochondria and lysosomes. Thirty minutes prior to acquiring the fluorescence images, mitochondria and lysosomes and were stained with Mitotracker Red CMXRos (final concentration, 100 nM) and Lysotracker blue (final concentration, 1μM), respectively (Invitrogen). After incubation, the cells were washed with serum free DMEM, and then observed by CLSM (FV10i-LIV; Olympus Corporation, Tokyo, Japan). The cells were excited with a 352 nm light, a 559 nm light and a 635 nm light from an LD laser. Images were obtained using an FV10i-LIV equipped with a water-immersion objective lens (UPlanSApo 60x/NA. 1.2) and a dichroic mirror (DM405/473/559/635). The three fluorescence detection channels (Ch) were set to the following filters: Ch1: 420/40 (blue) for Lysotracker blue, Ch2: Ch2: 570/50 (red) for Mitotracker Red CMXRos, Ch3: 660/50 (pseudo green) for Cy5-labeled ASO.

2.6 Immunostaining observation for mitochondrial protein using CLSM

R8/GALA-modified MITO-Porter encapsulating ASO (D-arm ASO [COX II] or D-arm Mock) (50 nM of total ASOs) were incubated with HeLa cells (1 x 10^5 cells/dish) seeded on 35

mm dishes in 1 mL of serum free DMEM for 3 hr under an atmosphere of 5 % CO_2/air at 37°C. The cells were washed with PBS, and further incubated in complete medium for 45 hr. Cells were fixed with 4% paraformaldehyde (10 min, room temperature) and incubated with 1% bovine serum albumin (BSA) (30 min, 37ºC). The cells were incubated with the rabbit anti-COX II antibody (used at 1:20 dilutions) and the mouse anti-SDHA antibody (used at 1:100 dilutions) for 24 hr at 4ºC. The anti-COX II and anti-SDHA antibody were detected by incubating the cells with goat anti-rabbit IgG Alexa488 (used at 1:100 dilutions) and goat anti-rabbit IgG Alexa568 (used at 1:100 dilutions) for 1 hr at 37ºC. Cells were analyzed by CLSM. The cells were excited with a 473 nm light and 559 nm light from an LD laser. Images were obtained using an FV10i-LIV equipped with a water-immersion objective lens (UPlanSApo 60x/NA. 1.2) and a dichroic mirror (DM405/473/559/635). The following filters were set to observation: Ch2: 490/50 (green) for goat anti-rabbit IgG Alexa488, Ch3: 570/50 (red) for goat anti-rabbit IgG Alexa568.

Relative COX II/SDHA protein expression levels were evaluated using Image Pro-Plus (Ropper Industries, Sarasota, FL) as described below. Fluorescent and bright-field cell images, after immunostaining by anti-COX II antibody (green) and anti-SDHA antibody (red), were captured using CLSM, as shown in Figure 4. Each eight-bit TIFF image was analyzed to quantify the total area of each region of interest. First, the yellow pixel areas where COX II proteins (green) were co-localized with mitochondria stained by anti-SDHA antibody (red) were marked in each image. The yellow and red pixel areas of each cluster in the cell, s_i(yellow) and s_i(red), were separately summed for each image, and are denoted as $S'_{z=j}$ (yellow) and $S'_{z=j}$ (red), respectively. The values of $S'_{z=j}$ (yellow) and $S'_{z=j}$ (red) in each image were further summed and are denoted as S(yellow) and S(red), respectively. These parameters represent the total area of COX II inside the mitochondria and the mitochondrial region in the total cell. Relative COX II/SDHA protein

expression levels was calculated as S(yellow) divided by S(red). This value was used to compare the relative variation in the expression of COX II protein among the carriers. Values for 64 individual cells were summarized for each treatment (Non treatment, D-arm Mock, D-arm ASO (COX II)) in Figure 5. The cells used in the analyses were chosen from images in multiple observations (n=6).

2.7 Observation of mitochondrial membrane potential using JC-1

R8/GALA-modified MITO-Porter encapsulating ASO (D-arm ASO [COX II] or D-arm Mock) (50 nM of total ASOs) were incubated with HeLa cells (1 x 10^5 cells/dish) seeded on 35 mm dishes in 1 mL of serum free DMEM for 3 hr under an atmosphere of 5% CO_2/air at 37°C. The cells were washed with PBS, and further incubated in complete medium for 45 hr. FCCP (a mitochondrial uncoupler) was used as a positive control for the down-regulation of mitochondrial membrane potential. In this experiment, the cells were treated with FCCP (final concentration, 100 μM) for sixty minutes prior to observation. Thirty minutes and ten minutes before acquiring the fluorescence images, the cells were stained with JC-1 (final concentration, 10 μM) to observe mitochondrial membrane potential and Hoechst 33342 (final concentration, 5 μg/mL) to stain nuclei, respectively. After the incubation, the cells were washed with serum free DMEM, and then observed by CLSM. The following filters were set to observation: Ch1: 455/50 (blue) for Hoechst 33342, Ch2: 490/50 (green) for monomeric form of JC-1, Ch3: 570/50 (red) for aggregated form of JC-1.

2.8 Statistical Analysis

The diameters, PDIs, and ξ-potentials of the carriers were measured. Each of the values shown in Table 1 (n=3) represent the mean ± S.D. Mitochondrial mRNA knockdown by the R8/GALA-modified MITO-Porter was evaluated. Each value shown in Figure 2 represents the mean ± SEM (n=3-4). Statistical significances between non treatment and others were calculated by one-way ANOVA, followed by the Dunnett test. Relative COX II/SDHA protein expression levels of each one cell were evaluated based on the images in Figure 4. In Figure 5, the values for 64 individual cells are summarized in each treatment and represented as circles, the mean (n=64) values are indicated by bars. Statistical significances between D-arm ASO [COX II] and others were calculated by one-way ANOVA, followed by Dunnett test. Levels of $p < 0.05$ were considered to be significant.

3. RESULTS

3.1 Construction of R8/GALA-modified MITO-Porter and evaluation of mitochondrial RNA knockdown

We evaluated the knockdown of mitochondrial mRNA, following the mitochondrial ASO delivery by R8/GALA-modified MITO-Porter. In this experiment, we used the D-arm modified antisense 2′-OMe RNA which targeted COX II (D-arm ASO [COX II]) (see Table S1 for details). We prepared R8/GALA-modified MITO-Porter encapsulating D-arm ASO [COX II] and D-arm-modified 2′-OMe RNA non-targeting COX II (D-arm Mock). The diameter, PDI (an indicator of particle-size distribution) and the ζ potential of the carriers are listed in Table 1. The envelope of

the carriers had a mitochondria-fusogenic composition [DOPE/SM/stearylated R8] [21, 22] equipped with Chol-GALA. As shown in Table 1, carriers with diameters less than 100 nm could be prepared with highly homogenous (PDI value of less than 0.20). The ζ potential of the carriers was ~40 mV. Based on these results, positively charged nanoparticles with homogenous structures were prepared in both the case of the R8/GALA-modified MITO-Porter (D-arm ASO [COX II]) and the R8/GALA-modified MITO-Porter (D-arm Mock).

After a 24 hr period of transfection by the R8/GALA-modified MITO-Porter, qRT-PCR, to detect the COX II (target mitochondrial mRNA) and ND I (control mitochondrial mRNA), was performed in order to evaluate the extent of knockdown of the target mitochondrial mRNA. As shown in Figure 2, a maximum of 40% knockdown of COX II was observed when the R8/GALA-modified MITO-Porter (D-arm ASO [COX II]) was used at a concentration of 250 nM, while the R8/GALA-modified MITO-Porter (D-arm Mock) had no effect on the mitochondrial mRNA levels of COX II. Moreover, mitochondrial RNA knockdown was not confirmed, when the ASO [COX II] without the D-arm was used (Figure S2). Thus, we conclude that a combination of the R8/GALA-modified MITO-Porter and the D-arm ASO [COX II] are involved in the knockdown of the target mitochondrial mRNA.

3.2 Intracellular observation of the R8/GALA-modified MITO-Porter

To verify that mitochondrial RNA knockdown was the result of the delivery of ASO to mitochondria by the R8/GALA-modified MITO-Porter, we observed the intracellular trafficking of the carrier using CLSM (Figure 3). In this experiment, the Cy-5 labeled D-arm ASO [COX II] was encapsulated in the R8/GALA-modified MITO-Porter. In the case of the R8/GALA-modified

MITO-Porter, numerous green and some yellow dots were observed in cells (Figures 3A, 3C), indicating that the Cy5-labeled ASOs (pseudo green color) were mainly localized in the cytosol and some ASOs were localized in red-stained mitochondria. To check endosomal escape efficiency, we observed the intracellular trafficking of the carriers after staining the acidic compartment blue (Figures 3B, 3C). The findings show that most of the green dots were observed to be outside the acidic compartment, suggesting that the carriers had been released from the endosomes to the cytosol. In the case of the R8-modified MITO-Porter without GALA, numerous cyan colored dots were observed in cells (Figure S3), indicating that the green-labeled cargoes were mainly localized in blue-stained acidic compartments. Collectively, the R8/GALA-modified MITO-Porter delivered the D-arm ASO [COX II] to mitochondria accompanied by endosomal escape, thus contributing to the knockdown of target mitochondrial mRNA. In the case of the Lipofectamine (LFN) RNAi MAX reagent, the cellular uptake of Cy5-labeled ASOs and the mitochondrial accumulation were lower than that for the R8/GALA-modified MITO-Porter, although the carriers would have been released from the endosomes to the cytosol (Figures. 3D-F). It was also confirmed that the transfection of the D-arm ASO [COX II] by the LFN RNAi MAX reagent did not decrease the target mitochondrial mRNA levels (date not shown), suggesting that ASOs in the cytosol does not affect mitochondrial knockdown.

3.3 Evaluation of protein knockdown by R8/GALA-modified MITO-Porter

We evaluated the variation in expression of target proteins after the mitochondrial delivery of ASO by the R8/GALA-modified MITO-Porter. Immunostaining was carried out to confirm the relative levels of target protein expression for an individual mitochondrion. COX II (target protein)

is a mitochondrial-encoded complex IV protein, while SDHA is a nuclear-encoded complex II protein, thus we used SDHA as a control protein. After a 48 hr period of transfection of the R8/GALA-modified MITO-Porter, HeLa cells were immunostained for COX II (green) and SDHA (red) and observed by CLSM (Figure 4). The green signals of target COX II protein was decreased by the administration of the R8/GALA-modified MITO-Porter (D-arm ASO [COX II]) (Figure 4G). On the other hand, the green signals when the D-arm Mock was transfected (Figure 4D) were comparable with those in non-treated cells (Figure 4A).

Moreover, we estimated the relative COX II/SDHA protein expression levels based on image analysis to evaluate the knockdown of the target protein by ASO transfection, as described in materials and methods. As a result, the use of the R8/GALA-modified MITO-Porter (D-arm ASO [COX II]) resulted in a significant decrease in COX II expression compared with transfection of D-arm Mock and non-treated cells (Figure 5). This image analysis also provided information to show that the relative COX II/SDHA protein expression levels were heterogeneous in individual cells. These results suggest that knockdown of target protein was observed by mitochondrial delivery of D-arm ASO [COX] using the R8/GALA-modified MITO-Porter.

3.4 Visualization of mitochondrial membrane potential after mitochondrial ASO delivery by R8/GALA-modified MITO-Porter

We evaluated the effect of ASO-mediated mitochondrial mRNA knockdown on the mitochondrial membrane potential. JC-1 is a cationic dye that exhibits a potential-dependent accumulation in mitochondria, as florescence emission shift from green (monomeric form) to red (aggregated form) [31]. The accumulation of JC-1 in normal mitochondria with a high

mitochondrial membrane potential, results in the production of a fluorescent red signal (Figure 6A), while a fluorescent green signal is produced in the case of mitochondria that have lost their mitochondrial membrane potential (Figure 6D). In this experiment, FCCP (a mitochondrial uncoupler) was used as a positive control for the down-regulation of mitochondrial membrane potential. After 48 hr transfection by R8/GALA-modified MITO-Porter, the HeLa cells were incubated with JC-1 and observed by CLSM. The fluorescent green signal of JC-1 was diffused into the cytosol in some cells by transfection of D-arm ASO [COX II] (Figure 6C), suggesting that the mitochondrial membrane potential was decreased. On the other hand, in the case of the transfection of D-arm Mock, red colored mitochondria are observed (Figure 6B), suggesting that R8/GALA-modified MITO-Porter itself does not affect the mitochondrial membrane potential. It was also confirmed that the use of the ASO [COX II] without the D-arm did not decrease the mitochondrial membrane potential (Figure S2). These results suggest that the D-arm ASO-mediated down regulation of COX II results in the inhibition in the mitochondrial respiratory chain.

4. Discussion

The findings reported herein provide a demonstration of the successful mitochondrial delivery and knockdown of target mRNA using a combination of a MITO-Porter system and D-arm ASO [COX II]. As mentioned in the introduction, the D-arm used in this study functions as a mitochondrial tRNA import signal and this sequence is imported into the mitochondrial matrix in mitochondria of *Leishmania* [27-29]. Thus, it would be expected that the D-arm would assist mitochondrial matrix delivery, even in human cells, as shown in Figure 1B. While, until decade ago, it was generally thought that tRNA is not imported into human mitochondria from the

cytoplasm, although the mitochondrial import of small RNAs had been demonstrated in a number of organisms. Tarassov and co-workers recently reported that some yeast tRNA derivatives can be imported into isolated human mitochondria [32]. They also showed that yeast $tRNA^{Lys}$ derivatives expressed in human cells are partially imported into mitochondria, and demonstrated the functionality of imported tRNAs in human mitochondria [33]. More recently, Rubio et al. reported that human mitochondria possess a similar active tRNA import system in vivo as well as other eukaryotes, and the import system is different from the protein import system [34].

Intracellular observations using CLSM permitted us to confirm that the R8/GALA-modified MITO-Porter succeeded in delivering cargoes to mitochondria in living cells (Figures 3A-C). To achieve this mitochondrial delivery, multiple processes including cellular uptake, endosomal escape and mitochondrial targeting need to be regulated, as shown in Figure 1A. We concluded that R8 and GALA were effective in regulating the intracellular trafficking to deliver the cargo to the target organelle. R8 functions as a cell-penetrating device that functions *via* macropinocytosis and a mitochondria-targeting peptide *via* electrostatic interaction. A previous report showed that the R8-modified MITO-Porter (conventional type) was efficiently internalized and escaped from macropinosomes to the cytosol with the encapsulated compounds being maintained intact, with the MITO-Porter being ultimately bound to mitochondria *via* electrostatic interactions [19, 20]. However, a detailed analysis of intracellular trafficking of R8-modified MITO-Porter revealed that the most of the carriers were localized in acidic compartments (endosomes and lysosomes), although the carriers were efficiently taken up by cells [21, 22]. The CLSM images shown in Figure S3 also indicate that the R8-modified MITO-Porter without GALA was mainly localized in acidic compartments. In this study, GALA was used to assist the carriers to escape from endosomes. Previously, it was reported that the inclusion of GALA in the surface

of liposomes promoted the destabilization of the endosomal membranes, thus enhancing endosomal escape [25]. Intracellular observations shown in Figures 3A-C and Figure S3 show that the R8/GALA-modified MITO-Porter had a higher endosomal escape efficiency than that of the R8-modified MITO-Porter (conventional type), resulting in higher mitochondrial targeting.

In the CLSM analysis, the R8/GALA-modified MITO-Porter (D-arm ASO [COX II]) was determined to be localized in the cytosol and mitochondria in the form of dots and not a diffuse form (Figures 3A-C), as previously reported [19, 20]. It was assumed that the D-arm ASO [COX II] was encapsulated in the carrier, and not decoated on the surface, after endosomal escape by GALA. In this form, the MITO-Porter delivered the D-arm ASO [COX II] to mitochondria via membrane fusion. While the LFN RNAi MAX reagent did not efficiently deliver the D-arm ASO [COX II] compared with the R8/GALA-modified MITO-Porter (Figures 3D-F). Adhya reported that a combination of a RNA import complex (RIC), a natural mitochondrial targeting carrier, and the D-arm of $tRNA^{Tyr}$, which was also used in our study, are important for successful mitochondrial delivery in human cells [35]. These results suggest that the D-arm derived from *Leishmania* would require the support of a mitochondrial targeting carrier for successful mitochondrial delivery in human cells, although only the D-arm can efficiently import cargoes into mitochondria of *Leishmania* [27-29]. Since little evidence exists for mitochondrial RNA import in human cells, this issue is deserving of further attention in the future.

Our results indicate that the R8/GALA-modified MITO-Porter delivered the D-arm ASO [COX II] to mitochondria, contributing to the knockdown of target mitochondrial mRNA and protein (Figures. 2, 4, 5). In mitochondria, post-transcriptional events appear to play a key role in the regulation of gene expression, and therefore RNA turnover is of particular interest [5, 7, 11].

double-strand RNA is disassembled in mitochondrial RNA degradosomes, which contain SUV3 and a polynucleotide phosphorylase [10-12]. Thus, the knockdown by mitochondrial delivery of D-arm ASO [COX II] would be induced not only via translational inhibition by the binding of target mitochondrial mRNA, but also by the degradation of the mitochondrial mRNA/D-arm ASO [COX II] duplex by RNA degradosomes. On the other hand, a combination of the R8/GALA-modified MITO-Porter and the ASO [COX II] without the D-arm failed to result in mitochondrial mRNA knockdown and had no effect on the mitochondria membrane potential (Figure S2). These results suggest that the D-arm might be required for the matrix import of ASO through the mitochondrial inner membrane. Thus, the MITO-Porter delivered the D-arm ASO [COX II] close to the mitochondrial inner membrane after fusion with the outer membrane, and the D-arm ASO [COX II] was then imported into the mitochondrial matrix via the D-arm import machinery, as shown in Figure 1B (upper part).

Our results also suggest that mitochondrial membrane potential was depolarized with down regulation of the respiratory chain as the result of the mitochondrial delivery of D-arm ASO [COX II]. The terminal step in the respiratory chain is the transfer of electrons from cytochrome c to oxygen to form water, a process that is catalyzed by complex IV of the respiratory chain. This electron transfer reaction helps to generate the mitochondrial membrane potential by pumping protons out of the matrix and ultimately driving ATP synthesis [36]. mtDNA-encoded subunits, COX I, COX II, and COX III, make up the catalytic core of complex IV [37, 38]. Interestingly, it was reported that mitochondria possess miRNA and that miR-181c regulates the gene expression of COX I by currently unknown post-transcriptional events [39]. An overexpression of miR-181c decreases the mRNA levels of COX I, resulting in an imbalance among the mitochondrially encoded subunits in complex IV, which has an effect on mitochondrial function (ex, an increased

production of reactive oxygen species) [39]. Thus, the knockdown of COX II by D-arm ASO [COX II] might induce a similar phenomenon, an imbalance among the subunits in complex IV, via the down regulation of COX I by miR-181c. It is therefore possible that this dysfunction of complex IV might have decreased mitochondrial membrane potential. In the future, we plan to use our nanocarrier to evaluate post-transcriptional events and functions including ATP induction and complex IV activity in mitochondria.

Judging from the images related to observing mitochondrial membrane potential by transfection using the R8/GALA-modified MITO-Porter (D-arm ASO [COX II]) (Figure 6), not all of the cells appear to have been transfected. In a previous study, we performed intracellular observations to evaluate the fraction of mitochondrial-targeted positive cells (transfected cells), and the conventional MITO-Porter transfected only a certain number of cells [21]. Therefore, it was presumed that the transfection of the R8/GALA-modified MITO-Porter would be heterogeneous. Consideration regarding this heterogeneous transfection would be supported by the results showing that the transfection of the D-arm ASO [COX II] achieved a sufficient knockdown of COX II at a concentration of 125 nM, while higher concentration of the D-arm ASO [COX II] did not result in a greater degree of knockdown (Figure 2). Moreover, imaging analyses to evaluate the relative levels of expression of the COX II/SDHA protein indicated that variations in the expression levels of the COX II protein were heterogeneous in individual cells (Figure 5). These results suggest that the fluorescent green signal of JC-1 might have diffused into the cytosol in certain cells, where the expression levels of COX II protein was lower than threshold value required to maintain mitochondrial membrane potential. These results indicate that a homogenous mitochondrial transfection technique is needed to establish a method to regulate mitochondrial gene expression.

5. Conclusion

Our finding constitutes the first report to demonstrate that the nanocarrier-mediated mitochondrial genome targeting of antisense RNA effects mitochondrial function. While, we were unable to determine whether this carrier would be able to achieve the specific knockdown of target mRNA, because the expression levels of all mitochondrial mRNA were not quantified. Further experiments including the validation of off-target effects and advanced function analysis will be required to establish a high-performance methodology for controlling mitochondrial gene expression and function. Future studies will involve detailed investigations of mitochondrial knockdown using a MITO-Porter system in conjunction with experts in the field of mitochondrial molecular biology.

Acknowledgement

This work was supported, in part, by the Program for Promotion of Fundamental Studies in Health Sciences of the National Institute of Biomedical Innovation, Japan (NIBIO) (project ID 10-62 to Y.Y.) and by a Grant-in-Aid for Young Scientists (A) (grant 23680053 to Y.Y.) and Scientific Research (S) (grant 22229001 to H.H.) from the Ministry of Education, Culture, Sports, Science and Technology of Japanese Government (MEXT). We thank Milton Feather for his helpful advice in writing the manuscript.

References

[1] Gomes-da-Silva LC, Fonseca NA, Moura V, Pedroso de Lima MC, Simoes S, Moreira JN. Lipid-based nanoparticles for siRNA delivery in cancer therapy: paradigms and challenges. Accounts of chemical research. 2012;45:1163-71.

[2] Huang L, Mollet S, Souquere S, Le Roy F, Ernoult-Lange M, Pierron G, et al. Mitochondria associate with P-bodies and modulate microRNA-mediated RNA interference. J Biol Chem. 2011;286:24219-30.

[3] Rubio MAT, Rinehart JJ, Krett B, Duvezin-Caubet S, Reichert AS, Soll D, et al. Mammalian mitochondria have the innate ability to import tRNAs by a mechanism distinct from protein import. P Natl Acad Sci USA. 2008;105:9186-91.

[4] Smirnov A, Comte C, Mager-Heckel AM, Addis V, Krasheninnikov IA, Martin RP, et al. Mitochondrial enzyme rhodanese is essential for 5 S ribosomal RNA import into human mitochondria. J Biol Chem. 2010;285:30792-803.

[5] Duchene AM, Pujol C, Marechal-Drouard L. Import of tRNAs and aminoacyl-tRNA synthetases into mitochondria. Curr Genet. 2009;55:1-18.

[6] Smirnov A, Entelis N, Martin RP, Tarassov I. Biological significance of 5S rRNA import into human mitochondria: role of ribosomal protein MRP-L18. Genes & development. 2011;25:1289-305.

[7] Bandiera S, Ruberg S, Girard M, Cagnard N, Hanein S, Chretien D, et al. Nuclear outsourcing of RNA interference components to human mitochondria. PloS one. 2011;6:e20746.

[8] Sripada L, Tomar D, Singh R. Mitochondria: One of the destinations of miRNAs. Mitochondrion. 2012;12:593-9.

[9] Liou GG, Jane WN, Cohen SN, Lin NS, Lin-Chao S. RNA degradosomes exist in vivo in Escherichia coli as multicomponent complexes associated with the cytoplasmic membrane via the N-terminal region of ribonuclease E. Proc Natl Acad Sci U S A. 2001;98:63-8.

[10] Wang DD, Shu Z, Lieser SA, Chen PL, Lee WH. Human mitochondrial SUV3 and polynucleotide phosphorylase form a 330-kDa heteropentamer to cooperatively degrade double-stranded RNA with a 3'-to-5' directionality. J Biol Chem. 2009;284:20812-21.

[11] Szczesny RJ, Borowski LS, Malecki M, Wojcik MA, Stepien PP, Golik P. RNA Degradation in Yeast and Human Mitochondria. Bba-Gene Regul Mech. 2012;1819:1027-34.

[12] Borowski LS, Dziembowski A, Hejnowicz MS, Stepien PP, Szczesny RJ. Human mitochondrial RNA decay mediated by PNPase-hSuv3 complex takes place in distinct foci. Nucleic acids research. 2013;41:1223-40.

[13] Miyata K, Nishiyama N, Kataoka K. Rational design of smart supramolecular assemblies for gene delivery: chemical challenges in the creation of artificial viruses. Chem Soc Rev. 2012;41:2562-74.

[14] Nakamura T, Akita H, Yamada Y, Hatakeyama H, Harashima H. A multifunctional envelope-type nanodevice for use in nanomedicine: concept and applications. Accounts of chemical research. 2012;45:1113-21.

[15] D'Souza GG, Rammohan R, Cheng SM, Torchilin VP, Weissig V. DQAsome-mediated delivery of plasmid DNA toward mitochondria in living cells. J Control Release. 2003;92:189-97.

[16] Lyrawati D, Trounson A, Cram D. Expression of GFP in the mitochondrial compartment using DQAsome-mediated delivery of an artificial mini-mitochondrial genome. Pharmaceutical research. 2011;28:2848-62.

[17] Seibel P, Trappe J, Villani G, Klopstock T, Papa S, Reichmann H. Transfection of mitochondria: strategy towards a gene therapy of mitochondrial DNA diseases. Nucleic acids research. 1995;23:10-7.
[18] Flierl A, Jackson C, Cottrell B, Murdock D, Seibel P, Wallace DC. Targeted delivery of DNA to the mitochondrial compartment via import sequence-conjugated peptide nucleic acid. Mol Ther. 2003;7:550-7.
[19] Yamada Y, Harashima H. Mitochondrial drug delivery systems for macromolecule and their therapeutic application to mitochondrial diseases. Adv Drug Deliv Rev. 2008;60:1439-62.
[20] Yamada Y, Akita H, Kamiya H, Kogure K, Yamamoto T, Shinohara Y, et al. MITO-Porter: A liposome-based carrier system for delivery of macromolecules into mitochondria via membrane fusion. Biochimica et biophysica acta. 2008;1778:423-32.
[21] Yamada Y, Furukawa R, Yasuzaki Y, Harashima H. Dual function MITO-Porter, a nano carrier integrating both efficient cytoplasmic delivery and mitochondrial macromolecule delivery. Mol Ther. 2011;19:1449-56.
[22] Yamada Y, Kawamura E, Harashima H. Mitochondrial-targeted DNA delivery using a DF-MITO-Porter, an innovative nano carrier with cytoplasmic and mitochondrial fusogenic envelopes. J Nanopart Res. 2012;14:1013-27.
[23] Khalil IA, Kogure K, Futaki S, Harashima H. High density of octaarginine stimulates macropinocytosis leading to efficient intracellular trafficking for gene expression. J Biol Chem. 2006;281:3544-51.
[24] Li W, Nicol F, Szoka FC, Jr. GALA: a designed synthetic pH-responsive amphipathic peptide with applications in drug and gene delivery. Adv Drug Deliv Rev. 2004;56:967-85.
[25] Kakudo T, Chaki S, Futaki S, Nakase I, Akaji K, Kawakami T, et al. Transferrin-modified liposomes equipped with a pH-sensitive fusogenic peptide: an artificial viral-like delivery system. Biochemistry. 2004;43:5618-28.
[26] Akita H, Kogure K, Moriguchi R, Nakamura Y, Higashi T, Nakamura T, et al. Reprint of: Nanoparticles for ex vivo siRNA delivery to dendritic cells for cancer vaccines: Programmed endosomal escape and dissociation. J Control Release. 2011;149:58-64.
[27] Mahapatra S, Ghosh S, Bera SK, Ghosh T, Das A, Adhya S. The D arm of tRNATyr is necessary and sufficient for import into Leishmania mitochondria in vitro. Nucleic acids research. 1998;26:2037-41.
[28] Bhattacharyya SN, Chatterjee S, Adhya S. Mitochondrial RNA import in Leishmania tropica: aptamers homologous to multiple tRNA domains that interact cooperatively or antagonistically at the inner membrane. Molecular and cellular biology. 2002;22:4372-82.
[29] Bhattacharyya SN, Mukherjee S, Adhya S. Mutations in a tRNA import signal define distinct receptors at the two membranes of Leishmania mitochondria. Molecular and cellular biology. 2000;20:7410-7.
[30] Sato Y, Hatakeyama H, Sakurai Y, Hyodo M, Akita H, Harashima H. A pH-sensitive cationic lipid facilitates the delivery of liposomal siRNA and gene silencing activity in vitro and in vivo. J Control Release. 2012;163:267-76.
[31] Reers M, Smiley ST, Mottola-Hartshorn C, Chen A, Lin M, Chen LB. Mitochondrial membrane potential monitored by JC-1 dye. Methods Enzymol. 1995;260:406-17.
[32] Entelis NS, Kolesnikova OA, Dogan S, Martin RP, Tarassov IA. 5 S rRNA and tRNA import into human mitochondria. Comparison of in vitro requirements. J Biol Chem. 2001;276:45642-53.

[33] Kolesnikova OA, Entelis NS, Jacquin-Becker C, Goltzene F, Chrzanowska-Lightowlers ZM, Lightowlers RN, et al. Nuclear DNA-encoded tRNAs targeted into mitochondria can rescue a mitochondrial DNA mutation associated with the MERRF syndrome in cultured human cells. Human molecular genetics. 2004;13:2519-34.
[34] Rubio MA, Rinehart JJ, Krett B, Duvezin-Caubet S, Reichert AS, Soll D, et al. Mammalian mitochondria have the innate ability to import tRNAs by a mechanism distinct from protein import. Proc Natl Acad Sci U S A. 2008;105:9186-91.
[35] Mukherjee S, Mahata B, Mahato B, Adhya S. Targeted mRNA degradation by complex-mediated delivery of antisense RNAs to intracellular human mitochondria. Human molecular genetics. 2008;17:1292-8.
[36] Chen JQ, Cammarata PR, Baines CP, Yager JD. Regulation of mitochondrial respiratory chain biogenesis by estrogens/estrogen receptors and physiological, pathological and pharmacological implications. Biochimica et biophysica acta. 2009;1793:1540-70.
[37] Capaldi RA, Marusich MF, Taanman JW. Mammalian cytochrome-c oxidase: characterization of enzyme and immunological detection of subunits in tissue extracts and whole cells. Methods Enzymol. 1995;260:117-32.
[38] Wu C, Yan L, Depre C, Dhar SK, Shen YT, Sadoshima J, et al. Cytochrome c oxidase III as a mechanism for apoptosis in heart failure following myocardial infarction. American journal of physiology Cell physiology. 2009;297:C928-34.
[39] Das S, Ferlito M, Kent OA, Fox-Talbot K, Wang R, Liu D, et al. Nuclear miRNA regulates the mitochondrial genome in the heart. Circulation research. 2012;110:1596-603.

Table 1. Physicochemical properties of R8/GALA-modified MITO-Porter.

	Diameter (nm)	PDI	ζ potential (mV)
R8/GALA-modified MITO-Porter (D-arm ASO [COX II])	85 ± 17	0.19 ± 0.04	36 ± 8
R8/GALA-modified MITO-Porter (D-arm Mock)	86 ± 14	0.19 ± 0.03	38 ± 8

Data denote the mean ± S.D.(n=3).

Figure 1. Schematic illustration of mitochondrial ASO delivery using the R8/GALA-modified MITO-Porter and mitochondrial RNA knockdown.

A, Intracellular trafficking of R8/GALA-modified MITO-Porter to reach to the mitochondria. Octaarginine (R8) functions as a cell-penetrating device via macropinocytosis and mitochondria-targeting peptide via electrostatic interaction. GALA, pH-sensitive and membrane fusogenic peptide, assists endosomal escape of the carriers. The R8/GALA-modified MITO-Porter is internalized by cells via macropinocytosis (1st step). Once inside the cell, the carrier escapes from the endosome into the cytosol by assistance of GALA (2nd step). The carrier then binds to mitochondria via electrostatic interactions with R8 (3rd step).

B, Conceptual image of the mitochondrial matrix delivery of ASO. After reaching to the mitochondria, D-arm (a mitochondrial tRNA import signal) modified ASO encapsulated in R8/GALA-modified MITO-Porter would facilitate mitochondrial matrix delivery as follows. One possibility is that the D-arm ASO is delivered to the IMS by the carrier via membrane fusion with the OM of a mitochondrion, and is then imported into the mitochondrial matrix via the D-arm import machinery (upper part). In the box for the D-arm ASO [COX II], bases in underlined italics are derived from the D-arm (see Table S1 for the detail). Another possibility is that the carrier directly introduces the D-arm ASO into the mitochondrial matrix through OM and IM on the contact sites of the mitochondrial membranes (lower part). IM, inner membrane; IMS, intermembrane space; OM, outer membrane.

C, Schematic image of mitochondrial mRNA knockdown and subsequent phenomena. In this experiment, the mRNA that codes for COX II was chosen as a target. COX II is one of mitochondrial proteins that make up complex IV of the respiratory chain. Under physiological conditions, mRNA of COX II is translated to the COX II protein, and it regulates mitochondrial function as a subunit of Complex IV (light part). If the knockdown (KD) of the target mRNA by mitochondrial delivery of D-arm ASO [COX II] was successful, the expression levels of target mitochondrial protein would be decreased, inducing an imbalance among the subunits in complex IV. Finally, a dysfunction in complex IV might not be able to regulate mitochondrial functions such as maintaining the mitochondrial membrane potential. D-arm ASO [COX II], D-arm modified antisense 2′-OMe RNA which targeted cytochrome c oxidase subunit II (COX II).

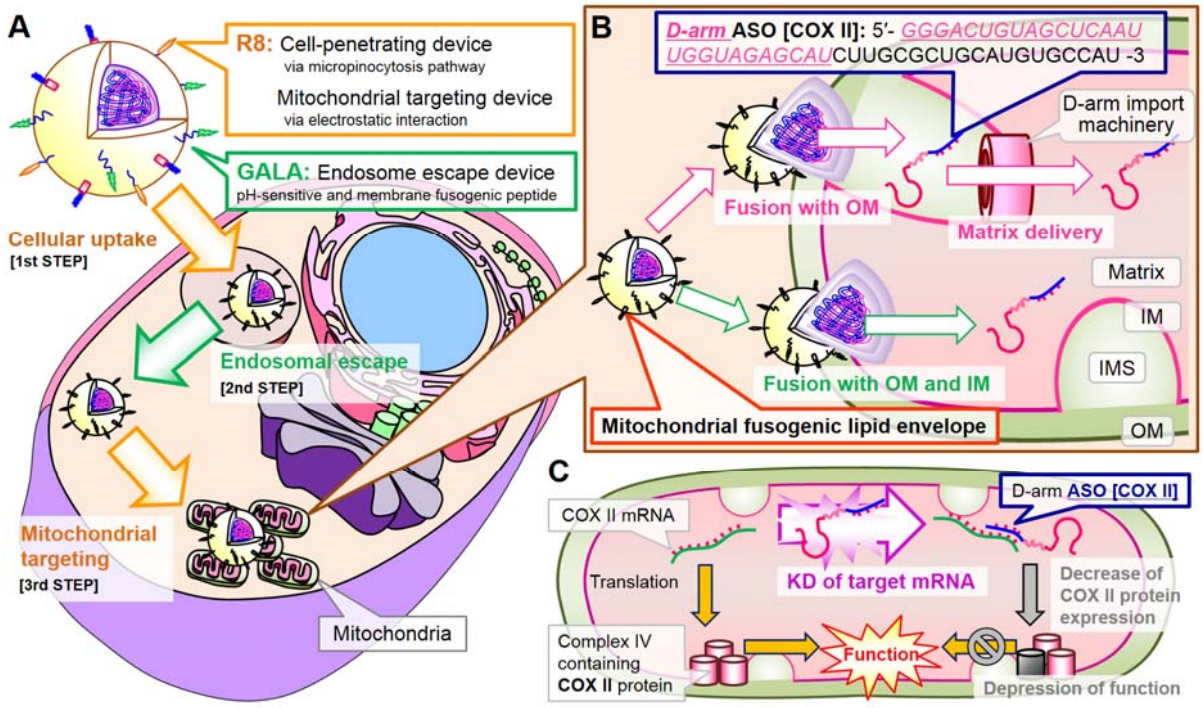
A
R8: Cell-penetrating device
via micropinocytosis pathway
Mitochondrial targeting device
via electrostatic interaction
GALA: Endosome escape device
pH-sensitive and membrane fusogenic peptide
Cellular uptake
[1st STEP]
Endosomal escape
[2nd STEP]
Mitochondrial targeting
[3rd STEP]
Mitochondria
B
D-arm ASO [COX II]: 5′- GGGACUGUAGCUCAAU UGGUAGAGCAUCUUGCGCUGCAUGUGCCAU -3
D-arm import machinery
Fusion with OM
Matrix delivery
Matrix
IM
IMS
Fusion with OM and IM
Mitochondrial fusogenic lipid envelope
OM
C
D-arm ASO [COX II]
COX II mRNA
Translation
KD of target mRNA
Decrease of COX II protein expression
Complex IV containing COX II protein
Function
Depression of function

Figure 2. Evaluation of mitochondrial mRNA knockdown by the R8/GALA-modified MITO-Porter.

After 24 hr transfection of R8/GALA-modified MITO-Porter, the knockdown effect of mitochondrial mRNA was evaluated by qRT-PCR. Bars indicates the mean with SEM (n=3-4). *Significant differences between Non treatment and others were calculated by one-way ANOVA, followed by the Dunnett test ($p<0.05$). COX II, cytochrome c oxidase subunit II.

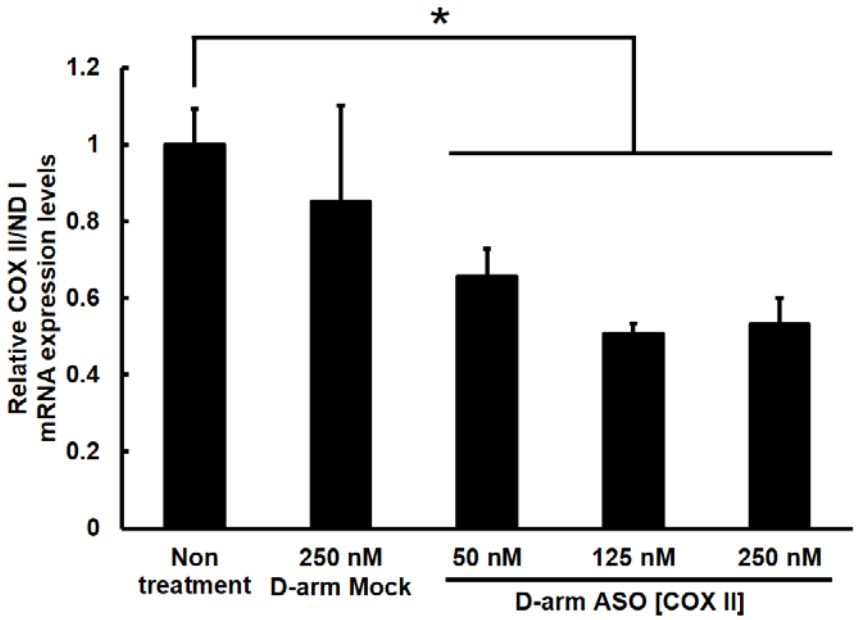

Figure 3. Intracellular observation of ASO after transfection by R8/GALA-MITO-Porter.

ASO encapsulated R8/GALA-modified MITO-Porter (A-C) and LFN RNAi MAX (D-F) were incubated with HeLa cells. Cy5-labeled D-arm ASO [COX II] (green pseudo color) was used for intracellular observations. Mitochondria and acidic compartments (e.g., endosomes and lysosomes) were stained with Mitotracker Red CMXRos (red) and LysoTracker Blue (blue), respectively. A, D indicates the merge image of the ASO and mitochondria. B, E indicates the merge image of the ASO and lysosome. C, F indicates the merged images of all fluorescence. Cy5-labeled D-arm ASO [COX II] appeared as yellow clusters (indicated with yellow arrows) when it was localized in mitochondria (A, C, D, F). Scale bars, 10 μm.

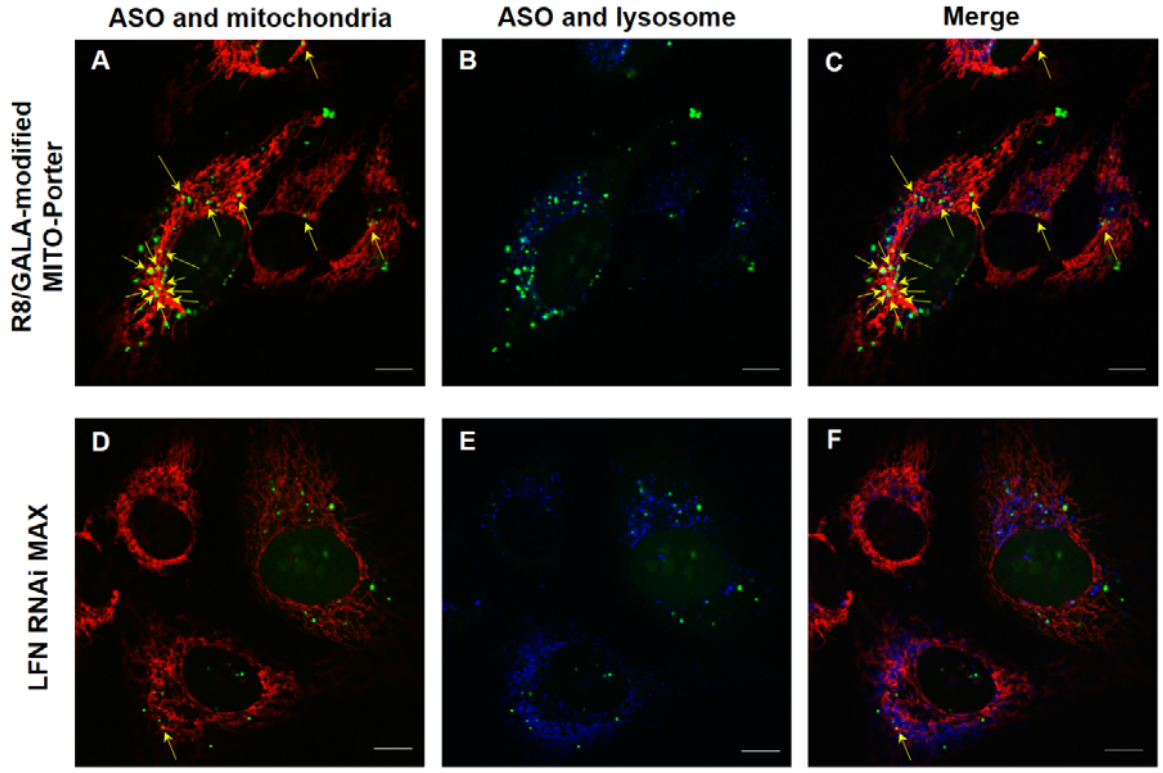

Figure 4. Immunostaining observation for mitochondrial protein knockdown by R8/GALA-modified MITO-Porter.

After 48 hr transfection of MITO-Porter, HeLa cells were incubated with anti-COX II antibody and anti-SDHA antibody, (A-C, Non treatment; D-F, D-arm Mock; G-I, D-arm ASO (COX II)).The cells were then observed by CLSM to detect COX II (green) and SDHA (red). Scale bars, 30 μm. COX II, cytochrome c oxidase subunit II; SDHA, succinate dehydrogenase complex subunit A.

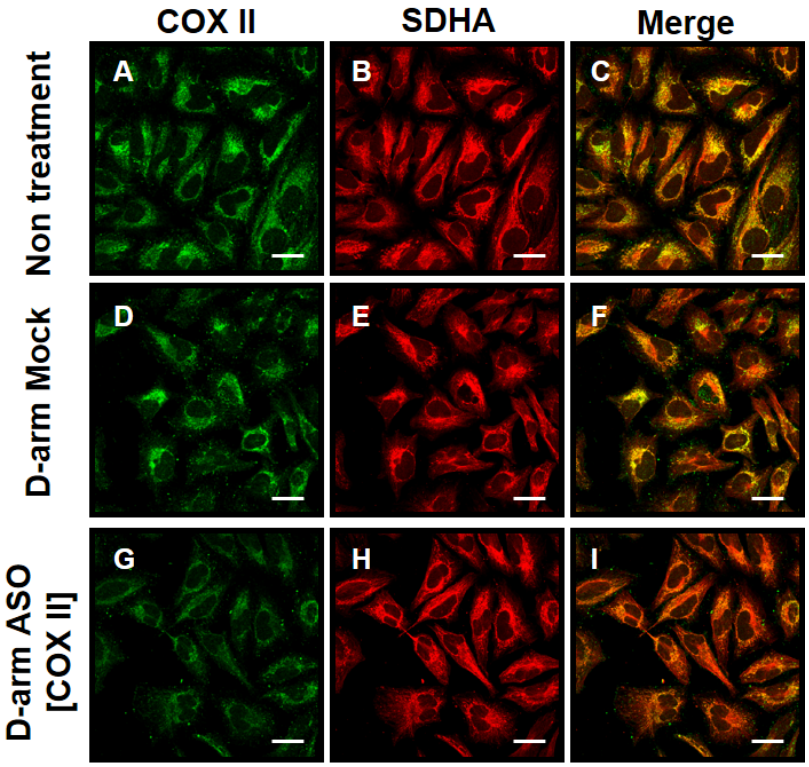

Figure 5. Evaluation of relative COX II/SDHA protein expression levels in mitochondrial protein knockdown.

Relative COX II/SDHA protein expression levels were evaluated based on the images in Figure 4, as described in material & methods. Circles represent the values of 64 individual cells summarized in each treatment. Bars are the mean value (n=64). **Significant differences between D-arm ASO [COX II] and others were calculated by one-way ANOVA, followed by Dunnett test ($p<0.01$). COX II, cytochrome c oxidase subunit II; SDHA, succinate dehydrogenase complex subunit A.

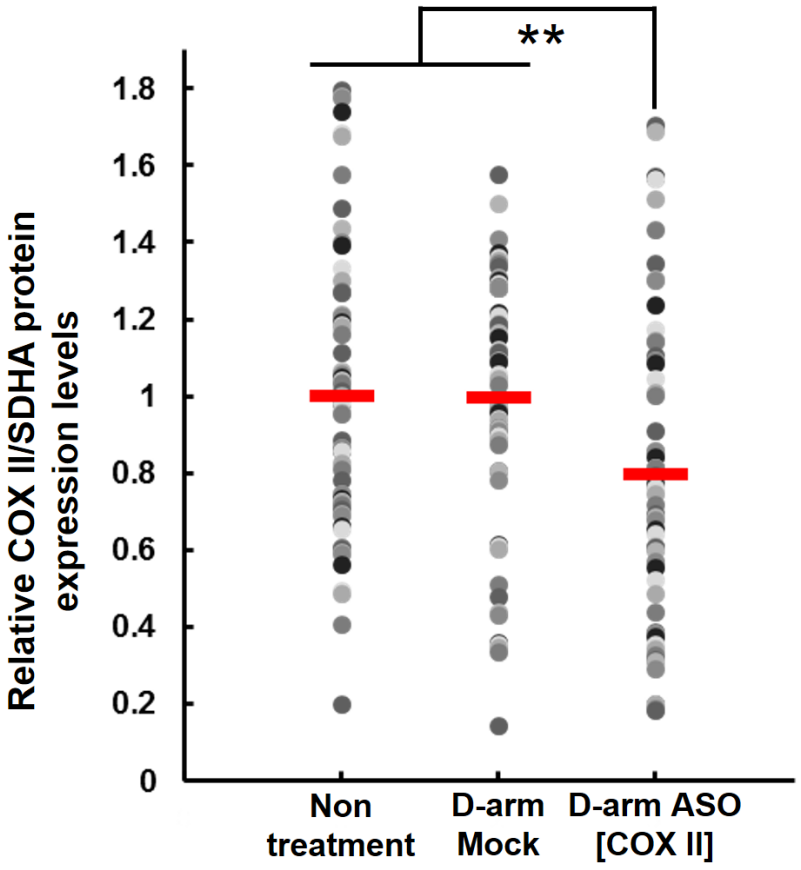

Figure 6. Visualization of mitochondrial membrane potential using JC-1.

After 48 hr transfection of R8/GALA-modified MITO-Porter (Non treatment (A), D-arm Mock (B), D-arm ASO (COX II) (C)), HeLa cells were incubated with JC-1 and observed by CLSM. FCCP is an uncoupling reagent used as a positive control for the down-regulation of mitochondrial membrane potential (D). Scale bars, 30 μm. COX II, cytochrome c oxidase subunit II; FCCP, carbonyl cyanide 4-(trifluoromethoxy) phenylhydrazone.

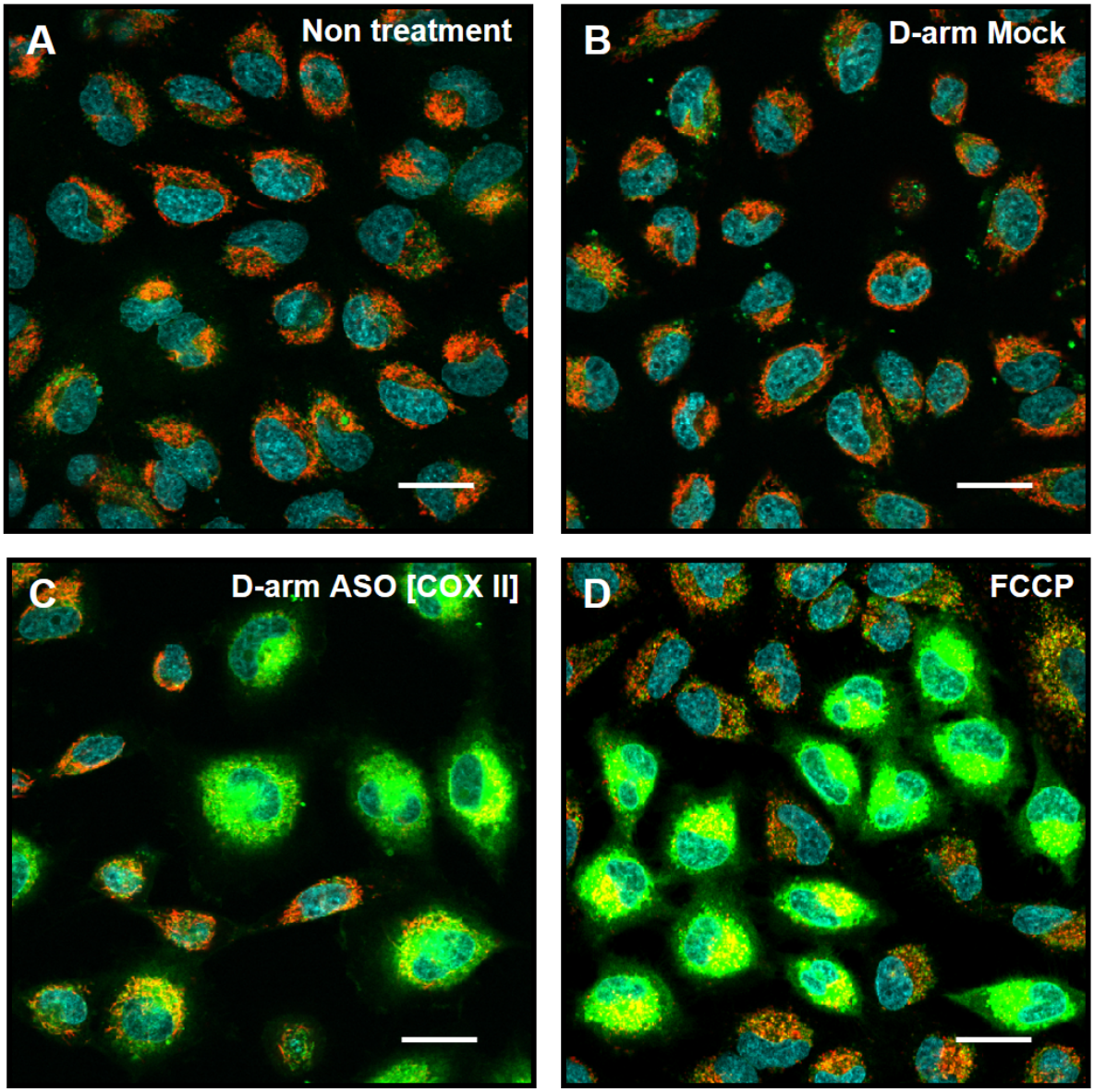

Supplementary data

Figure S1. Gel images of the RT–PCR detection of mitochondrial mRNA coding COX II in HeLa cells.

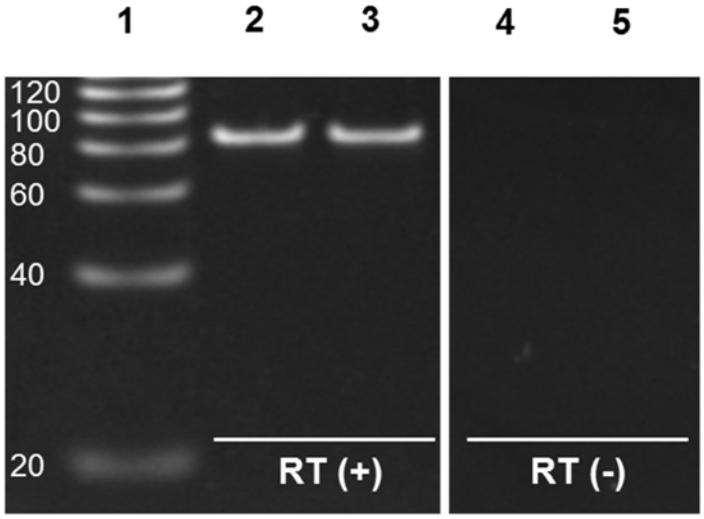

Total RNA was purified by RNeasy and PCR was done with specific primers for mitochondrial mRNA coding COX II ((forward) 5′- ATCATCCTAGTCCTCATCG -3′ and (reverse) 5′- GATTTGATGGTAAGGGAGG -3′) after reverse transcription (RT (+), lanes 2,3) and before reverse transcription (RT (-), lanes 4,5). The PCR products were detected by ethidium bromide staining after separation by electrophoresis. Lane 1, 20 bp DNA Ladder; lanes 2,4, Non-treatment; lanes 3,5, treated with HEPES buffer.

Figure S2. Evaluation of mitochondrial mRNA knockdown and observation of the mitochondrial membrane potential after transfection of the non-D-arm ASO [COX II] by the R8/GALA-modified MITO-Porter.

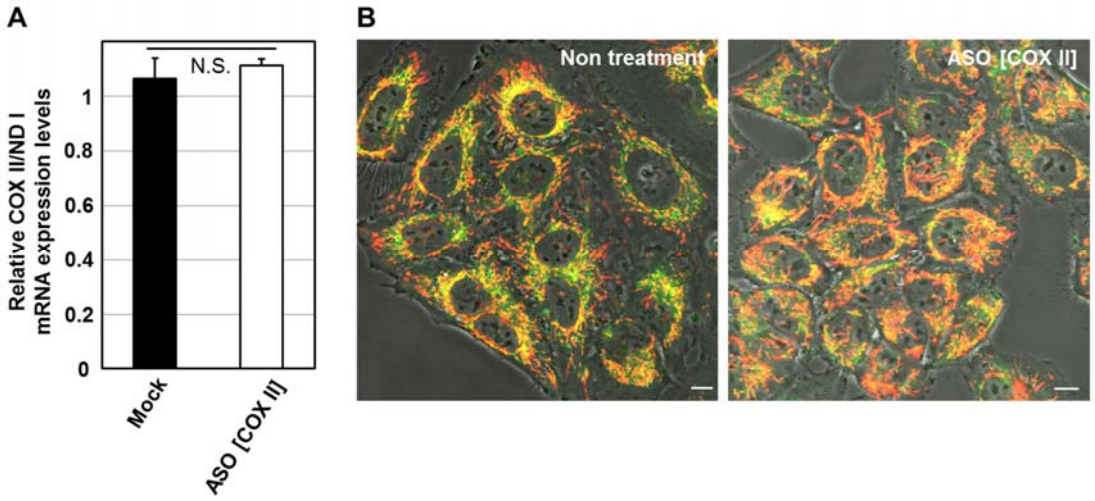

(**A**) Evaluation of mitochondrial mRNA knockdown. After 24 hr of transfection by ASO [COX II] or Mock, which contain no D-arm, using the R8/GALA-modified MITO-Porter (250 nM of total ASOs), the knockdown effect of mitochondrial mRNA was evaluated by qRT-PCR. Data are represented as the mean ± SEM (n=3). We performed unpaired Student's t test. N.S., no significant differences were observed.

(**B**) Observation of mitochondrial membrane potential. After 48 hr of transfection by ASO [COX II], which has no D-arm, using the R8/GALA-modified MITO-Porter (50 nM of total ASOs), HeLa cells were incubated with JC-1 and observed by CLSM under similar condition as Figure 6. Scale bars, 10 μm. COX II, cytochrome c oxidase subunit II.

Figure S3. Intracellular observation of R8-modified MITO-Porter (conventional type) using CLSM.

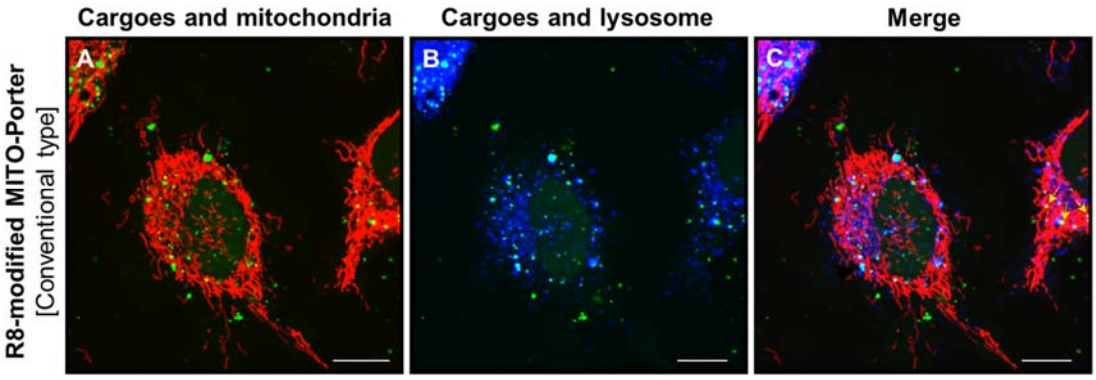

The R8-modified MITO-Porter was incubated with HeLa cells. FAM-labeled 2′-OMe RNA (5-CGACGGAGGUUGGCCAUGGGUAUGUCGUCG-3, green color) was used as a cargo for the intracellular observations. Mitochondria and acidic compartments (e.g., endosomes and lysosomes) were stained with Mitofluor 589 (red) and LysoTracker Blue (blue), respectively. A indicates the merged image of the cargoes and mitochondria. B indicates the merged image of the cargo and lysosome. C indicates the merged images of all fluorescence. FAM-labeled 2′-OMe RNA appears as yellow clusters (indicated with yellow arrows) when it was localized in mitochondria (A, C), while it appears as cyan clusters when localized in lysosomes (B, C). Scale bars, 10 μm.

Table S1. RNA oligonucleotide used in this study.

RNA oligonucleotide	[a] Nucleotide sequence	Property
D-arm ASO [COX II]	5′- **GGGACUGUAGCUCAAUUGGUAGA GCAU***CUUGCGCUGCAUGUGCCAU* -3′	**D-arm modified** antisense 2′-OMe RNA which *targeted COX II*
D-arm Mock	5′- **GGGACUGUAGCUCAAUUGGUAGA GCAU**CGACAAGCGCACCGAU -3′	**D-arm-modified** 2′-OMe RNA non-targeting COX II
ASO [COX II]	5′- *CUUGCGCUGCAUGUGCCAU* -3′	D-arm-unmodified antisense 2′-OMe RNA which *targeted COX II*
Mock	5′- CGACAAGCGCACCGAU -3′	D-arm-unmodified 2′-OMe RNA non-targeting COX II

[a] Bases in underlined bold are derived from the D-arm and italics are antisense sequence targeted to a region in the mRNA of cytochrome c oxidase subunit II (COX II).